Harmonic Suppression of Three-Phase Four-Wire Inverter

Menglong Wei[1(✉)], Yanhui Guo[2], and Sheng Dong[3]

[1] School of Electrical Engineering, Beijing Engineering Research Center of Electric Rail Transportation, Beijing Jiaotong University, Beijing 100044, China
20121505@bjtu.edu.cn
[2] New Line Business Department of Beijing Metro Operation Co. Ltd., Beijing 100044, China
[3] The Second Project Management Center of Beijing Rail Transit Construction Management Co. Ltd., Beijing 100044, China

Abstract. With the development of rail transit technology, auxiliary inverter which is as an important on-board power supply equipment faces more and more kinds of load equipment. Especially the nonlinear load (such as frequency conversion air conditioning) seriously affects the voltage quality of auxiliary power supply of trains. In the current research of auxiliary inverter control, the effect of 100% nonlinear load control is not good. In this paper, an improved resonant converter is introduced, which can suppress the specific subharmonics very well and has a relatively simple form. The model of the auxiliary inverter is established by MATLAB, and the control algorithm is verified.

Keywords: Improved resonant controller · Nonlinear load · Auxiliary inverter

1 Introduction

In the double closed loop system, rational configuration of current inner loop parameters can enhance the ability of system with impact loads, but control of the nonlinear load and unbalanced load ability is weak, in order to solve this problem, predecessors have put forward many feasible method:

PID control is widely used and the technology is relatively mature, but it cannot realize the control of AC quantity without static difference, and the control ability of nonlinear load is not strong [1].

The deadbeat control is a control technology based on discrete mathematical model. It has a good control effect on the nonlinear negative and auxiliary general systems. However, the error between the actual output voltage and the reference voltage is not zero, and the switching frequency is not fixed [2].

Based on the inner membrane principle, the repetitive control can suppress all the subharmonics in theory, but it is not effective and has poor stability [3].

The resonant controller is also based on the inner membrane principle, which can realize the no-static control of the AC quantity. Its complexity leads to some difficulties in the parameter design. However, because of its incomparable advantages in handling harsh loads, a new resonant controller is proposed in this paper [4].

L. Jia et al. (Eds.): EITRT 2021, LNEE 864, pp. 225–231, 2022.
https://doi.org/10.1007/978-981-16-9905-4_27

2 Conventional Resonant Controller

The basic idea in the derivation process of traditional resonant controller is to transfer the integral controller in the DQ coordinate system to the static coordinate system, so that no difference adjustment can be realized in the static coordinate system, as shown in Fig. 1.

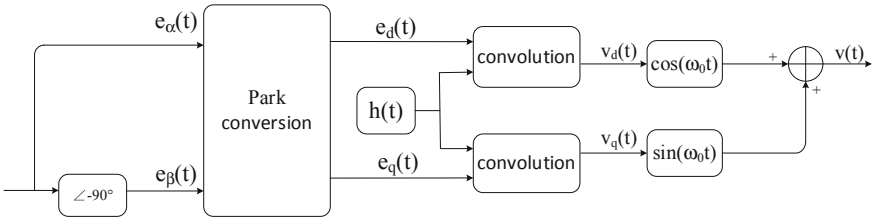

Fig. 1. Conventional resonant controller

The traditional single-phase inverter controller derivation block diagram is as Fig. 1, where e(t) represents the difference between the instruction value and the feedback value, h(t) represents the controller, and v(t) represents the control result. After delay, e(t) transforms the original single-phase AC quantity into two intersect flows under the αβ axis, which is transformed into direct flows under the dq coordinate system through Park transformation [7]. In this way, h(t) can be controlled without static error only by selecting an integrator, and finally the control results can be converted into single-phase AC quantity. Therefore, the transfer function of the traditional resonant controller can be deduced as shown in the formula (1).

$$G_R(s) = \frac{K}{2}[H(s + jw_0) + H(s - jw_0)] = \frac{Ks}{s^2 + w_0^2} \tag{1}$$

The traditional resonant controller and the proportional controller are generally composed of the proportional + resonant controller. In this way, the high bandwidth and high dynamic performance can be realized through the proportional controller, and the specific frequency sub-characteristics can be controlled by the resonant controller. However, the mode of proportional control + resonant controller also increases the complexity of the control system. Moreover, the proportional + resonant controller has a large low-frequency gain, poor attenuation ability to DC bias, and a large phase lag, which is not conducive to the configuration of the inverter equivalent output impedance [8]. Therefore, a new type of resonant controller can be designed, which has better DC bias attenuation ability and less phase lag, which is easy to design control parameters, and has a strong ability to suppress output voltage distortion caused by nonlinear load. Combining the advantages and disadvantages of the above methods, the new resonant converter is shown in the Fig. 2 below:

Compared with the traditional resonant controller, the improved resonant converter simplifies the Park transformation process. It can be obtained from the figure:

$$v(t) = e(t)\cos(w_0 t) \otimes h(t)\cos(w_0 t) + e(t)\sin(w_0 t) \otimes h(t)\sin(w_0 t) \tag{2}$$

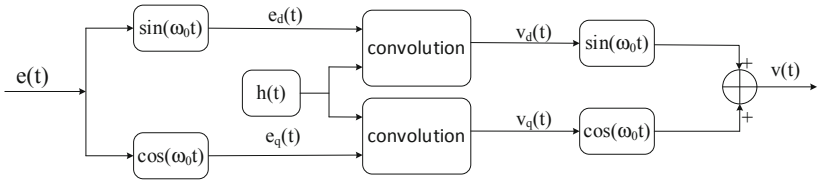

Fig. 2. Improved resonant converter

The Laplace transform of Eq. (2) can be obtained:

$$\begin{aligned} V(s) &= \frac{1}{2}H(s)[E(s+jw_0)+E(s-jw_0)] \otimes \frac{s}{s^2+w_0^2} \\ &+\frac{1}{2j}H(s)[E(s+jw_0)+E(s-jw_0)] \otimes \frac{s}{s^2+w_0^2} \end{aligned} \tag{3}$$

It can be simplified as follows:

$$V(s) = \frac{1}{2}[H(s+jw_0)E(s)+H(s-jw_0)E(s)] \tag{4}$$

Equation (4) shows that the results obtained by the improved resonant converter are the same as those obtained by the traditional resonant converter, and the above equation can more simply explain the derivation process of the resonant controller, and its physical significance is clear [6].

The improved resonant controller is different from the traditional resonant controller in which h(t) is a simple integrator, but the coupling effect of the dq axis is taken into account ($j\omega_0$ term is introduced to offset the coupling), and a proportional controller is introduced to improve the controller gain, as shown in the following formula:

$$\begin{cases} H(s-jw_0) = \frac{1}{s-jw_0} \Rightarrow H(s-jw_0) = K_{pr} + K_{ir}(1+jw_0)\frac{1}{s-jw_0} \\ H(s+jw_0) = \frac{1}{s+jw_0} \Rightarrow H(s+jw_0) = K_{pr} + K_{ir}(1-jw_0)\frac{1}{s+jw_0} \end{cases} \tag{5}$$

In order to adjust the gain at the resonant frequency more conveniently, a damping effect that only acts on the resonant frequency gain is introduced, as shown in Eq. (6).

$$\begin{cases} K_{pr} + K_{ir}(1+jw_0)\frac{1}{s-jw_0} \Rightarrow K_{pr} + K_{ir}(1+jw_0)\frac{w_c}{s+w_c-jw_c} \\ K_{pr} + K_{ir}(1-jw_0)\frac{1}{s+jw_0} \Rightarrow K_{pr} + K_{ir}(1-jw_0)\frac{w_c}{s+w_c+jw_c} \end{cases} \tag{6}$$

Substituting Eq. (6) into Equation (4), we can get:

$$G(s) = \frac{2[K_{pr}s^2 + (K_{ir}+2K_{pr})w_c s + (K_{ir}+K_{pr})w_c^2 + (K_{pr}-K_{ir}w_c)w_0^2]}{s^2+2w_c s+w_c^2+w_0^2} \tag{7}$$

Equation (7) is too complex and has defects in the control performance. For example, when one of the parameters is adjusted, the characteristics in the full frequency band will change, which is not conducive to the reasonable configuration of the controller

parameters. Under ideal conditions, parameter adjustment should only affect part of the frequency band characteristics, and achieve decoupling between various parameters of the controller, so as to improve the pertinence of the adjustment process. In addition, the low-frequency gain of the above equation is large, and it cannot effectively attenuate the DC bias in the control quantity [5]. Therefore, the final form of the improved controller can be obtained by reasonably optimizing Eq. (8):

$$G_R(s) = \frac{K_{pr}s^2 + K_{ir}s}{s^2 + 2w_c s + w_0^2} \tag{8}$$

3 Simulation

The traditional photo controller Bert is shown in the Fig. 3. From the observation of the figure, it can be found that changing K can only affect the overall gain, and the gain at the low frequency band and the resonant point cannot be adjusted separately, which will cause inconvenience to the application of the resonant controller.

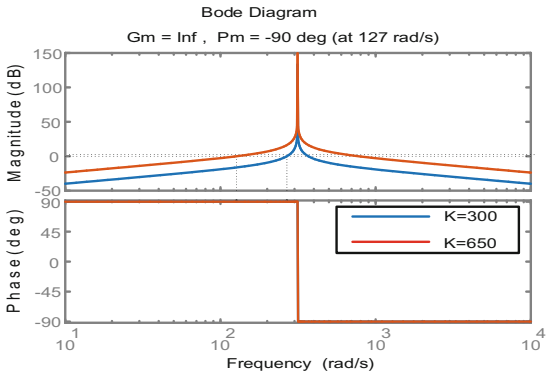

Fig. 3. Bode diagram of traditional resonant controller

As shown in Fig. 4, the modified resonant controller parameters change bode diagram, chart can be seen that the original form of the modified resonant controller all the defects have been corrected, for example due to low frequency attenuation control can quickly gain small volumes of dc bias, change the omega c only gain effect on resonant frequency, without affecting the other spectrum characteristics, Changing K_{ir} only affects the characteristics of low frequency band, but does not affect other frequency band characteristics. Therefore, if you want to adjust a part of the characteristics, only need to modify the specific parameters, more simple and convenient.

MATLAB software is used for simulation. The inverter adopts three-phase four-wire structure, and the double closed-loop control strategy of the system is shown as follows:

The control strategy shown in Fig. 5 is characterized by double closed-loop control, three-phase separate control of voltage loop, and the modes of PID + fundamental

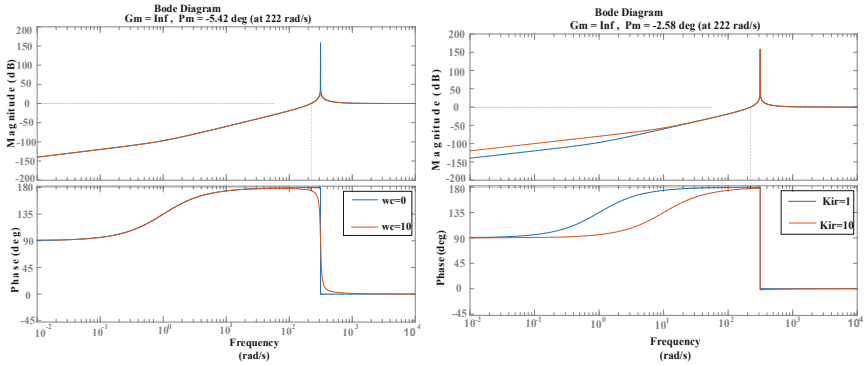

Fig. 4. Bode diagram of an improved resonant controller

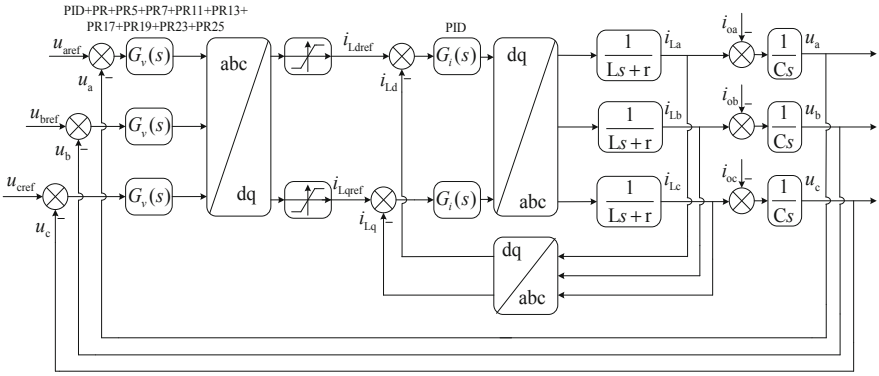

Fig. 5. Single machine control strategy

resonance controller + 5, 7, 11, 13, 17 and 19 resonance controllers for each voltage controller respectively. After passing through the voltage loop, the current loop instruction is obtained. The current loop instruction needs to be transformed to the DQ coordinate system. The feedback quantity of current loop adopts inductive current, and the current instruction value is limited to the amplitude of 1.3 times the rated current, which is used to realize the short-circuit operation of 10 s. The current loop controller adopts PID controller.

The Fig. 6 above shows the output waveform of 120 kW nonlinear load, channel 1 is the phase voltage waveform, channel 2 is the output current waveform, channel 3 is the line voltage waveform, and channel 4 is the DC side voltage waveform.

Figure 7 shows the 120 kW nonlinear load voltage THD waveform, in which the THD of the basic resonant controller is 13.27%, and the THD of the special resonant controller is 8.83%. It can be seen from the figure that the 5th to 19th harmonics have been basically eliminated, demonstrating the effectiveness of the designed resonant controller.

The resonant controller has the most obvious control effect under the 120 kW nonlinear load. The Table 1 shows the THD comparison of different resonant controllers, and

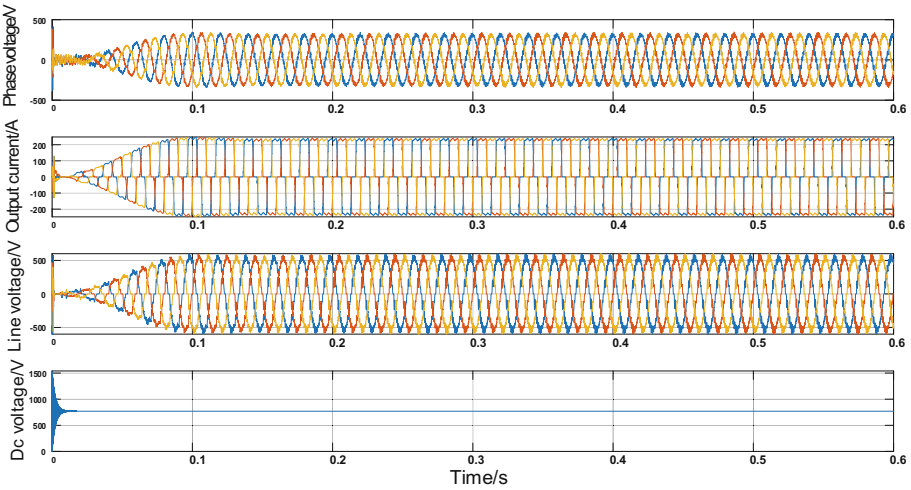

Fig. 6. 120 kW nonlinear load voltage and current waveform

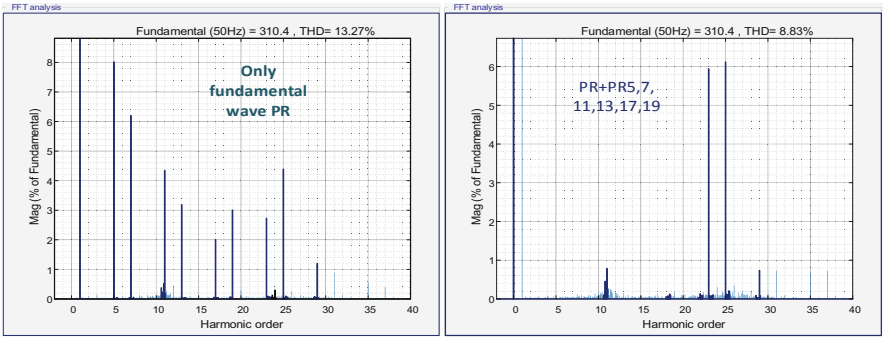

Fig. 7. 120 kW nonlinear load THD

the control effect of each resonant controller on each harmonic can be seen. PR stands for fundamental resonant controller only, PR5 stands for quintic resonant controller, and others are similar.

Table 1. Comparison of THD output voltages of different controllers

Different sub-resonant controllers	Phase voltage THD/%	Line voltage THD/%
PR	13.27	13.01
PR + PR5,7	11.28	11.17
PR + PR5,7,11,13,17,19	8.83	8.55

4 Conclusion

In this paper, the harms and research status of nonlinear load in recent years are introduced, and the advantages of the improved resonant controller over the traditional resonant controller are illustrated. Based on this, the voltage and current double closed-loop model is designed. Moreover, the model and simulation of the inverter control system are carried out by using MATLAB/Simulink tool, and the effectiveness of the improved resonant controller is verified.

Acknowledgments. This work was supported by the Fundamental Research Funds for the Central Universities under Grant 2018JBM055.

References

1. Abdel-Rahim, N.M., Quaicoe, J.E.: Analysis and design of a multiple feedback loop control-strategy for single-phase voltage-source UPS inverters. Power Electron. IEEE Trans. **11**(4), 532–541 (1996)
2. Chen, J.: Research on High-quality Waveform Control and Key Technology of Unconnected Line Parallel in Auxiliary Power Supply System of Urban Rail Train. Beijing Jiaotong University (2013). (in Chinese)
3. Ryan, M.J., Brumsickle, W.E., Lorenz, R.D.: Control topology options for single-phase UPS inverters. Ind. Appl. IEEE Trans. **33**(2), 493–501 (1997)
4. Hornik, T., Zhong, Q.C.: A current-control strategy for voltage-source inverters in microgrids based on H(infinity) and repetitive control. IEEE Trans. Power Electron. **26**(3), 943–952 (2011)
5. Keliang, Z., Danwei, W., Bin, Z., et al.: Plug-In dual-mode-structure repetitive controller for CVCF PWM inverters. Ind. Electron. IEEE Trans. **56**(3), 784–791 (2009)
6. Mattavelli, P., Marafao, F.P.: Repetitive-based control for selective harmonic compensation in active power filters. Ind. Electron. IEEE Trans. **51**(5), 1018–1024 (2004)
7. Castilla. M., Miret, J., Camacho, A., et al.: Reduction of current harmonic distortion in three-phase grid-connected photovoltaic inverters via resonant current control. Ind. Electron. IEEE Trans. (2011)
8. Ke, S., Jianze, W., Zhiqiang, G., et al.: Dynamic Voltage Restorer Based on Proportional-resonant Control. Power and Energy Engineering Conference (APPEEC), pp. 1–4. Asia-Pacific (2010)